[6] Vaglio-Laurin, R., "Laminar heat transfer on three-dimensional blunt nosed bodies in hypersonic flow," ARS J. **29**, 123–129 (1959).

[7] Hayes, W. D. and Probstein, R. F., *Hypersonic Flow Theory* (Academic Press Inc., New York, 1959).

[8] Hayes, W. D. and Probstein, R. F., "Viscous hypersonic similitude," J. Aerospace Sci. **26**, 815–824 (1959).

[9] Cohen, C. B. and Reshotko, E., "Similar solutions for the compressible laminar boundary layer with heat transfer and pressure gradient," NACA TR 1293 (1956).

[10] Reshotko, E. and Beckwith, I., "Compressible laminar boundary layer over a yawed infinite cylinder with heat transfer and arbitrary Prandtl number," NACA TN 3986 (1957).

[11] Lighthill, M. J., "On displacement thickness," J. Fluid Mech. **4**, 383–392 (1958).

[12] Weyl, H., "On the differential equations of the simplest boundary layer problems," Ann. Math. **43**, 381–407 (1942).

[13] Bloom, M. H. and Steiger, M. H., "Perturbed boundary-layer solutions applied to the wall jet and Blasius profile," *Developments in Mechanics* (Plenum Press, Inc., New York, 1961), Vol. I.

[14] Janowitz, G. and Libby, P. A., "The effect of variable transport properties on a dissociated boundary layer with surface reaction," Polytechnic Institute of Brooklyn, PIBAL Rept. 804 (October 1963); also Int. J. Heat Mass Transfer (to be published).

[15] Hayday, A. A., "Mass transfer cooling in a laminar boundary layer in steady two-dimensional stagnation flow," Univ. of Minnesota, TN 19, Air Force Office of Scientific Research AFOSR TN 58-337, AD 154 241 (1958).

[16] Hoshizaki, H. and Smith, H. J., "The effect of helium injection at an axially symmetric stagnation point," J. Aerospace Sci. **26**, 399–400 (1959).

[17] Syvertson, C. A. and McDevitt, J. B., "Effects of mass addition on the stability of slender cones at hypersonic speeds," AIAA J. **1**, 939–940 (1963).

JANUARY 1965 AIAA JOURNAL VOL. 3, NO. 1

Magnus Characteristics of Finned and Nonfinned Projectiles

ANDERS S. PLATOU*
Ballistic Research Laboratories, Aberdeen Proving Ground, Md.

This is a summary of the Magnus force and moment measurements obtained on finned and nonfinned projectiles during the past several years. Most of the measurements have been obtained in the Ballistic Research Laboratories' (BRL) supersonic wind tunnels, with a few measurements taken in the BRL transonic range and the Naval Ordnance Laboratory's wind tunnels. The results have provided considerable insight into the generation of the Magnus force and moments on both finned and nonfinned projectiles. For nonfinned bodies at small angles of attack, having a laminar boundary layer, the Magnus force, at least on short bodies, obeys Martin's theory. At high angles of attack the Magnus force can be estimated from the lift force on a spinning cylinder flying perpendicular to the flow. The Magnus force on a spinning finned projectile is composed of two forces: a body force and a fin force. The forces normally act in opposite directions, thereby tending to cancel one another. However, the forces do not act at the same location; therefore a Magnus moment is created which is nearly independent of the center of gravity position. There are also two other known sources of Magnus moments on finned bodies which are created under certain conditions. These conditions are defined in this paper and the magnitude of the moments are estimated.

Nomenclature

a = speed of sound
b = fin span
d = major model diameter (also see Fig. 19)
r = radius of model or distance from center of rotation
c = fin chord
l = model length
M = Mach number $= U/a$
P_0 = stagnation pressure
P_b = fin base pressure
P_∞ = freestream static pressure
q = dynamic pressure $\frac{1}{2}\rho U^2 = \frac{1}{2}\gamma P_\infty M^2$
R_e = Reynolds number $\rho Ud/\mu$
R_l = Reynolds number $\rho Ul/\mu$
T_0 = stagnation temperature
t = fin thickness
U = freestream velocity
U_c = projectile cross velocity $U_c = U \sin\alpha$
S = body cross-sectional area $\pi d^2/4$
S_b = fin base area
A = body longitudinal cross-sectional area
y = radial distance from body centerline to fin cross section
α = angle of attack
α_B = body angle of attack
δ = fin angle of cant
ρ = freestream density
μ = freestream viscosity
ω = spin rate of model (plus is clockwise looking upstream)
ν = $\omega r/U$ or $\omega d/2U$
c.p. = Magnus force center of pressure from base
c.g. = center of gravity
C_L = lift force coefficient L/qS
C_N = normal force coefficient N/qS
$C_{N\alpha}$ = $dC_N/d\alpha$
C_m = pitching moment coefficient m/qSd
$C_{m\alpha}$ = $dC_m/d\alpha$
C_f = Magnus force coefficient $f/qS\nu$ (plus is to left looking upstream)
$C_{f\alpha}$ = $dC_f/d\alpha$
C_T = Magnus moment coefficient $T/qSd\nu$ (plus is plus force ahead of moment center)
$C_{T\alpha}$ = $dC_T/d\alpha$

Introduction

THE aerodynamic forces acting on a nonfinned body of revolution in free flight can only be influenced by spin through the viscous properties of the surrounding boundary

Received March 25, 1964; revision received June 12, 1964.
* Research Engineer, Supersonic Wind Tunnels. Member AIAA.

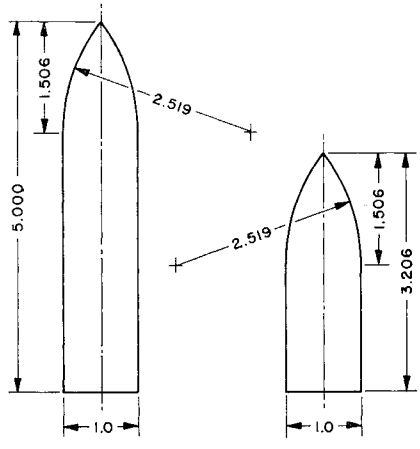

Fig. 1 3.2- and 5-caliber bodies.

layer. The body surface velocities due to spin impart a velocity to the adjacent air, thereby altering the boundary-layer properties. In particular, the boundary-layer thickness distribution is altered so that the effective aerodynamic shape of the body is changed. The effective body shape will remain symmetric at zero angle of attack so that no influence on the aerodynamic forces, except possibly drag, is expected until the body assumes an angle of attack other than zero.

The principal result of the realignment of the boundary-layer properties due to spin is a force acting perpendicular to the angle of attack plane. This force in ballistic nomenclature is called the Magnus force† and it will be the principal force discussed in this article. (The normal force and pitching moment, which were also measured during this investigation, are not affected by spin within the accuracy of our measurements.) The Magnus force is a small force and in all cases measured to date is less than 5% of the normal force. However, the force and its associated moment about the body center of gravity can be very important in predicting projectile behavior.

The Magnus force on a finned body is produced by an entirely different mechanism. As is explained in this paper, rotating fins can produce Magnus forces and moments which are much larger than the body Magnus forces and moments. The usual assumption that Magnus effects can be neglected because the spin is small is erroneous. These Magnus moments are shown in this paper to be produced by at least three separate unrelated phenomena.

Nonfinned Bodies

Magnus Force at Low Angles of Attack

In the preliminary analysis of the Magnus force on a nonfinned body of revolution at small angles of attack we consider a simple streamlined body surface containing no discontinuities. The boundary-layer growth is uniformly increasing along the body, and the complete boundary layer can be pictured as a thin shell completely enclosing the body except at the base. This shell effectively alters the aerodynamic shape of the body and influences the generated aerodynamic forces. For a nonspinning body, the boundary-layer shell is symmetric about the angle-of-attack plane, and no mechanism is present for producing side (Magnus) forces or moments. On a spinning body, the thin shell will have viscous forces transmitted to it which will destroy the angle-of-attack plane symmetry. This distorted shell or aerodynamic body is then able to produce side (Magnus) forces and moments. Experimental proof of this idea at low speeds has been obtained at Guggenheim Aeronautical Laboratory, California Institute of Technology (GALCIT).[2]

Martin,[3] using the preceding ideas, has developed an expression for the Magnus force and its center of pressure. The three-dimensional boundary-layer equations for the cylindrical portion of a body of revolution are solved for small angles of attack and small spin rates. The boundary-layer velocity components are used to compute the variation in displacement thickness produced by spin and the Magnus force, and its centers of pressure are computed using the slender body theory on the resulting asymmetric body. The main assumptions are a slender open-ended hollow circular cylinder for the body, low angle of attack, incompressible flow, and a laminar boundary layer. In applying the theory to a typical body of revolution, one must make allowances for the length of the nose. Martin suggests using an effective cylinder length equal to the body cylinder length plus one-half the nose length. The expressions developed by the theory are

$$C_{f\alpha} = (52.6/R_l^{1/2})(l/d)^2 \qquad \text{c.p.}/l = 0.40$$

Kelly and Thacker[4, 5] have extended the theory to include a radial pressure gradient effect and a skin-friction term. They also consider the next higher-order terms in spin which make the Magnus force nonlinear in spin. Their results are as follows:

$$C_{f\alpha} = \frac{8(l/d)^2}{(R_l)^{1/2}}\left[7.834 - 16.526\left(\frac{\omega d}{2U}\right)^2\left(\frac{l}{d}\right)^2 + \ldots .\right]$$

$$\text{c.p.}/l = 0.40 + 0.375(\omega d/2U)^2(l/d)^2 + \ldots .$$

The status of the boundary layer is also a very important parameter in predicting the Magnus force. The velocity distribution in the layer and the displacement thickness are controlling factors, and each of these is a function of the previous history of the boundary layer. Laminar boundary layers have different velocity profiles and thicknesses from turbulent boundary layers so that the spin influence on each type may be different. In fact, the properties of various turbulent layers will depend on their previous histories, such as the location and cause of transition, so that the spin influence may differ for various turbulent boundary layers.

Experimental verification of the forementioned ideas, using the bodies shown in Fig. 1, are presented in Table 1 and Figs. 2 and 3. In order to obtain laminar boundary layers, it is necessary to test at low Reynolds numbers where the aerodynamic forces are small because of the low dynamic pressures. This reduces the accuracy of the data, especially at the higher Mach numbers, and decreases the reliability of the laminar

Table 1 Laminar boundary-layer data

M	$R_l \times 10^{-6}$	$C_{f\alpha}$ theory	$C_{f\alpha}$ exper.	c.p. theory, caliber from base	c.p. exper., caliber from base
		3.2-caliber body			
1.57	1.85[a]	0.235[a]	0.281	0.98[a]	0.75
2.00	1.58[a]	0.255[a]	0.276	0.98[a]	1.0
2.47	1.58[a]	0.255[a]	0.321	0.98[a]	1.25
3.02	1.58[a]	0.255[a]	0.337	0.98[a]	1.0
		5-caliber body			
1.75	1.55[b]	0.76[b]	0.88	1.7[b]	1.75
2.00	1.40[b]	0.80[b]	0.75	1.7[b]	2.0
3.00	1.29[b]	0.84[b]	0.97	1.7[b]	2.25

[a] Based on $l/d = 2.45$.
[b] Based on $l/d = 4.25$.

† Named after G. Magnus, who first predicted its presence in 1852.[1]

boundary-layer data. Because of this, the general conclusion on the agreement of experiment with theory is that Martin's theory predicts the right order of magnitude for short bodies (3 to 5 caliber) with laminar boundary layers. In all cases so far measured, it is believed that the data are accurate within 10 to 20%.

It was impossible to obtain data on the 3.2-caliber body having a turbulent boundary layer produced by natural transition. Natural transition is dependent on the exact surface details around the periphery of the body and, on the 3.2-caliber body, transition did not occur at the same axial location around the body surface. While the body is spinning, the force caused by irregular transition will average out; however, at zero spin, the side force will depend on the roll orientation of the model. Since a constant zero spin reading is essential,[6] it is necessary to fix transition by artificial means. However, artificial transition may create slightly different conditions than those occurring with natural transition. Also, the boundary-layer characteristics are different in that the velocity profile and the thickness may change. Therefore, it is unknown whether the measured Magnus data with artificial transition are representative of natural transition. To partially overcome this deficiency, three sizes of trip rings, located $\frac{3}{4}$ caliber from the nose, were used to create turbulent boundary layers having different characteristics. (Each of the trip rings was several times larger than the laminar boundary-layer thickness.) The Magnus data obtained under these conditions (Fig. 2) show that 1) the Magnus force is linear with angle of attack and spin, and 2) the Magnus force is dependent on the boundary-layer characteristics. Therefore, it is impossible to predict the force, within close tolerances, unless one knows the exact boundary-layer conditions. Since a wide range of trip sizes were used, it is very possible that the Magnus force on any short body having a turbulent boundary layer will be within the range shown here.

The 5-caliber body surface details were sufficiently smooth so that only small variations in the side force occurred because of zero spin roll orientation of the body. This indicates that the transition location is nearly independent of roll position at zero spin, and zero spin readings could be obtained without resorting to artificial transition. However, the added length of the 5-caliber body made it necessary to decrease the Reynolds number in order to obtain a completely laminar boundary layer. This in turn decreases the tunnel dynamic pressure and the measured force. Fortunately the Magnus force obeyed Martin's theory so that the additional body

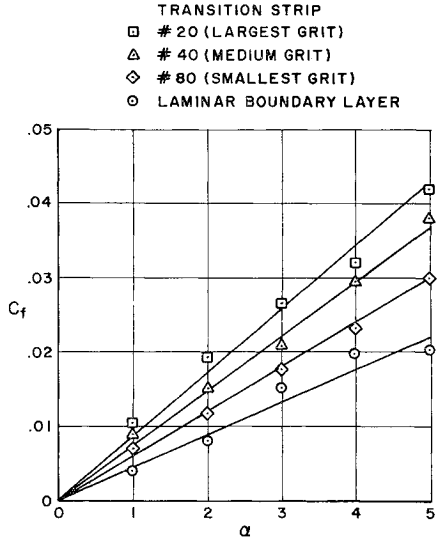

Fig. 2 Effect of boundary layer on the Magnus force of the 3.2-caliber body: $M = 2.0$, $Re = 0.65 \times 10^6$.

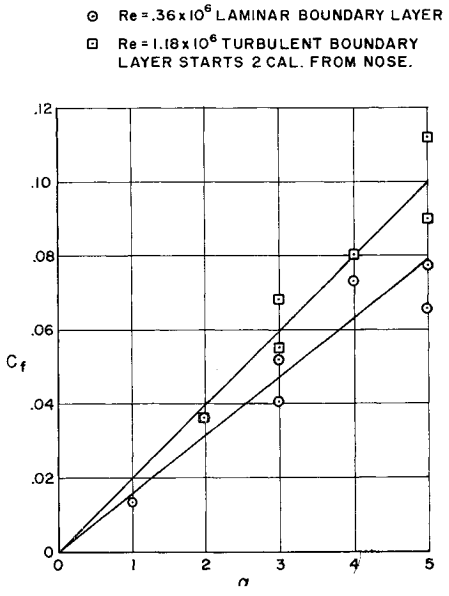

Fig. 3 Effect of boundary layer on the Magnus force of the 5 caliber body: $M = 1.75$.

length increased the Magnus force, thereby more than offsetting the decreased Reynolds number effect. Some of the 5-caliber data are shown in Fig. 3.

As with the 3.2-caliber body, the Magnus force on the 5-caliber body is linear with spin and angle of attack and is also dependent on the boundary-layer characteristics. The turbulent boundary layer creates a larger Magnus force than the laminar boundary layer. However, the transition location and the turbulent boundary layer are very Reynolds-number sensitive, and it is expected that Magnus force variations will also occur with Reynolds number. If higher Reynolds number data could be obtained, it is expected that data similar to that obtained on the 3.2-caliber body, with artificial transition (Fig. 2), would result. Therefore, it is impossible, from the existing data, to determine the exact Magnus force that would exist on these bodies unless the exact boundary-layer conditions are known. It can only be said that a larger Magnus force can be expected when a turbulent boundary layer exists on the body.

The laminar boundary-layer data can be compared with Martin's theory. This is done in Table 1 and it can be seen that good agreement is obtained on both configurations. The theoretical $C_{f\alpha}$ is computed using the half nose length suggested by Martin. Zero and full nose length were also used, but the half nose length gave the best comparison. Considering the limitations of the theory and the data accuracy, the agreement is good for both force and center of pressure. This indicates that the Magnus force coefficient varies as the square of the body length and inversely as the square root of the Reynolds number. These data also indicate that $C_{f\alpha}$ is independent of spin and do not agree with the Kelly-Thacker results shown earlier.

The center of pressure data obtained on these bodies (Fig. 1) are not sufficiently accurate to pinpoint the force under various conditions. However, it is possible to state that under all conditions tested the measured center of pressure is aft of the forward moment gage (2.25 calibers forward of the base for the 3.2-caliber body and 2.88 calibers for the 5-caliber body) and in most cases it is located on the aft third of the body so that changes in the nose configuration should not influence the force, except through possible changes in the boundary-layer characteristics. No conclusions on the motion of the center of pressure with angle of attack and spin can be made because of the inaccuracy of the data.

Most shells or bullets that are fired from guns require modifications to the streamlined shape of Fig. 1 in order that

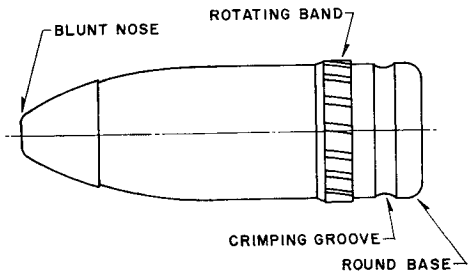

Fig. 4 Modifications of the streamlined shape shown in Fig. 1.

they may be successfully launched. These modifications, in most cases, create discontinuities in the body surface which complicate the flow field and the boundary layer and in turn complicate the resulting Magnus force. No theory is available for predicting the effect of spin under these conditions.

In order to determine the effect of some of these modifications, we ran experiments on the series of configurations having discontinuities like those shown in Fig. 4. Each of the configurations tested contained one or more of the discontinuities so that the effect of each discontinuity could be ascertained. The results are quite different from the previous linear results and, surprisingly enough, the simplest modification gives the most nonlinear results. Rounding the corner of the base gives the results shown in Fig. 5. The Magnus force is not only nonlinear with spin and angle of attack, but is also negative for a portion of the spin and angle-of-attack range. This applies for both types of boundary layer. The mechanism that produces the negative force is not completely understood; however, it may be because of a change in flow separation points on the round base caused by spin. A numerical computation of the pressure difference required on the round portion of the base to produce the difference in Magnus force has been made. The pressure difference is approximately 0.004 times the stagnation pressure, whereas the static pressure at the base is approximately 0.10. This means that only a small pressure change is required to account for the change in Magnus force, and it is entirely feasible that this pressure difference could be produced by separation on the round base. These small pressure differences would not be observed in schlieren photographs.

A similar experiment[7] carried out in the BRL aerodynamics range verifies, to some extent, the wind-tunnel round base result. Two shell configurations, identical except for a square or hemispherical base, show a difference in Magnus moments (Fig. 6) which could be attributed to a negative force acting on the hemispherical base. The Magnus force was not obtained during these tests, so that the moment difference could also be attributed to a shift in the centers of pressure.

Data on configurations having the other discontinuities are not quite so surprising. The blunt nose has very little effect, whereas the rotating band and crimping groove decrease the Magnus force slightly. The combined effect of all the modifications is to add to the negative effect of the round base and provide a configuration having considerable negative force. See Refs. 6 and 8 for additional data on these configurations.

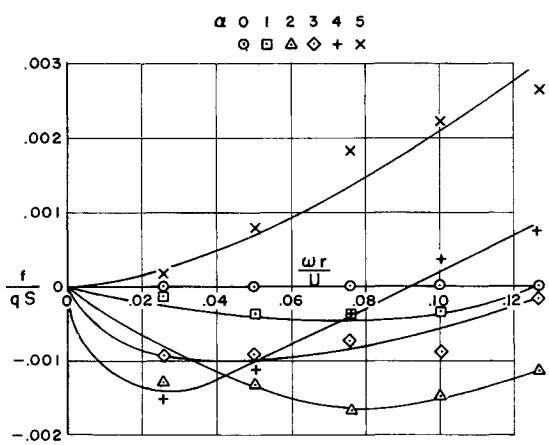

Fig. 5 Magnus force on the 3.2 caliber body with a round base: $M = 2.0$, $Re = 0.65 \times 10^6$, number 40 transition strip.

Magnus Force at High Angles of Attack

At high angles of attack, the source of the Magnus force is probably entirely different from that depicted by Martin. The boundary layer is no longer a thin shell around the entire body surface, as at low angles of attack, but is interrupted by the wake on the lee side of the body. This makes the concept of an asymmetric thin boundary-layer shell, as proposed by Martin at low angles of attack, impossible, and so we must attempt to look at the problem from a new viewpoint.

The normal forces on nonrotating bodies at high angles of attack are reasonably well described, using the ideas of Allen[9] and Kelly.[10] If we apply these ideas to the prediction of the Magnus force at high angles of attack, we have to relate the Magnus force on a given section of body to the Magnus force on a spinning cylinder oriented normal to the flow. The normal velocity for each section is taken to be the component of the freestream velocity normal to the body axis. Further, the Magnus force on the sections have to be related, not to the steady-state Magnus forces on a cylinder, but rather to the force on a rotating cylinder, impulsively started from rest before it has developed the steady-state force. The forces on forward body sections correspond to short travel distances, and the rearward body sections to relatively larger travel distances for the cylinder. If the body is long enough, the steady-state forces will probably be reached. Unfortunately, the low-speed starting data are not available and would be very difficult to obtain. At large freestream Mach numbers and high angles of attack, the cross Mach number will approach and may exceed unity. In this case, even the low-speed starting data would not be sufficient, for as soon as transonic velocities are reached in the cross-flow, the law of the forbidden signal restricts the field of influence of the body spin.

At low freestream speeds, the cylinder rotation causes the boundary-layer separation to differ on the top and bottom of the cylinder. As a result, the vorticity of opposite sign shed at the top and bottom is not equal, and there is a net amount of vorticity shed in the cylinder wake. As this happens, an equal but opposite amount of circulation is developed about the whole cylinder, and the pressure distribution over the whole cylinder is altered, resulting in a Magnus force. When the flow is supersonic, the circulation cannot

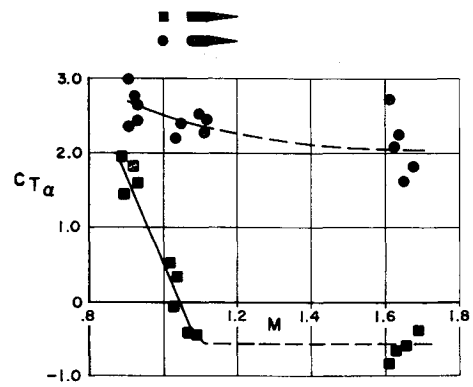

Fig. 6 Magnus moments for the shell of Ref. 7.

develop over the whole cylinder, so that the effects of unequal vortex shedding must be restricted to the wake, except for possible shifting of the separation points. The Magnus force must then be caused only by changes in pressure over the rear portion of the cylinder. Because the field of influence is restricted by the forbidden signal rule, it is suspected that the Magnus force might be dependent on the cross Mach number. Also, the Magnus force on a highly inclined body might be comparable to the Magnus force on a rotating cylinder mounted perpendicular to the flow.

To determine this, we recomputed all of the Magnus force coefficients available on bodies of revolution so that the coefficient is based on the body cross velocity ($U \sin\alpha$) and the body longitudinal cross-sectional area. (The Magnus data include Naval Ordnance Laboratories (NOL) data,[11] as well as BRL data.) These coefficients are plotted in Fig. 7, and it is seen that above $M = 0.6$ the Magnus force decreases as the cross Mach number increases. A comparison of these data with data obtained on a rotating cylinder[12] mounted normal to a transonic or supersonic stream (Fig. 7) shows that an approximate correlation exists between the two sets of data above $M = 0.8$. The correlation shows that it is possible to predict the Magnus force on simple bodies of revolution in cases where the cross Mach number is 0.8 or higher.

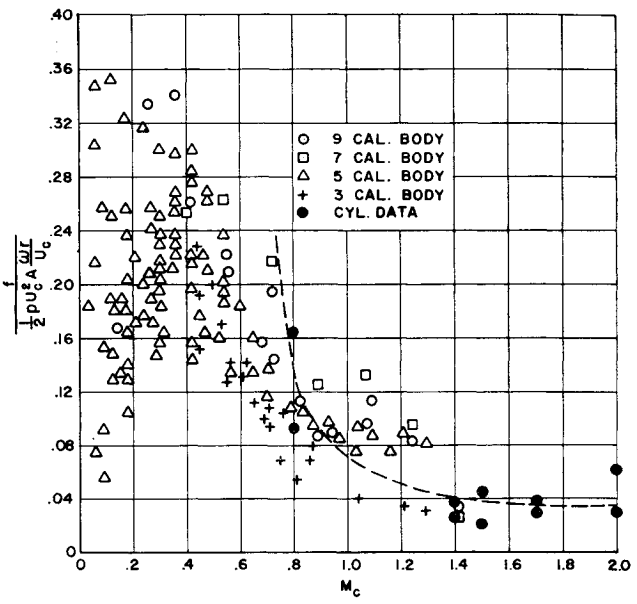

Fig. 7 Magnus force vs the cross flow Mach number.

Finned Bodies

In many cases of finned projectile flights, it has become necessary to spin the projectile during flight in order to overcome the manufacturing asymmetries of the fins. This tends to nullify the effect of fin asymmetry; on the other hand, the spin does impart a Magnus force and moment to the projectile which may be significant. The bare-body Magnus force has been explained in the preceding section; however, the influence of spin on the fins is a different phenomena. In fact, three entirely unrelated phenomena caused by spin have been found which can influence the aerodynamic forces and moments on fins.

Magnus Effects Due to Body-Fin Interference

When a rectangular flat plate traveling at a velocity U is rotated at a rate ω, about a line parallel to one of its sides, a lift force is generated which is equal to

$$C_L = 4\alpha/(M^2 - 1)^{1/2}$$

Here M is the freestream Mach number and α is the angle of attack created by the rotation of the flat plate. α varies uniformly along the span of the flat plate, and has its largest value at the tip chord section $\alpha = \omega r/U$.

When there is a series of flat plates aligned as the fins on a projectile, the lift force on each fin contributes toward a torque about the centerline of rotation (the body axis) which tends to retard the rotation. The lift on each fin is perpendicular to the fin surface, and at zero angle of attack the lift forces on opposite fins cancel one another. When the projectile is at other than zero angle of attack, the body interference on the fins is such that the lift force on the leeward fin is reduced, thereby leaving an unbalanced force. This force acts perpendicular to the angle-of-attack plane. From Fig. 8 it can be seen that this force acts in the opposite direction from the body Magnus force. It is therefore possible, depending on the body and fin configuration, to obtain either a positive, zero, or negative Magnus force on the projectile. The behavior of the Magnus force in this case can only be determined by finding the body interference from experiments.

Even though the body and fin Magnus forces oppose one another, they do not have the same center of pressure. As a result, a moment couple is created which is equal to the lesser of the two forces multiplied by the distance between the two forces (Fig. 8). The Magnus moment about the projectile center of gravity will be the sum of the couple plus the moment due to the unbalanced Magnus force.

In many cases, the fins of a projectile are canted, so that the projectile will free spin during flight. When this occurs, the lift distribution on each fin and, in turn, the Magnus force, becomes more complicated than on the uncanted fin. Ignoring tip effects, when the projectile is at zero angle of attack, the lift distribution on each fin is

$$dL = C_{L_\alpha}\alpha q\, cdr = C_{L_\alpha}[(\omega r/U) - \delta]q\, cdr$$

When the fin is free spinning,

$$\int rdL = 0 = C_{L_\alpha}qc \int_{r_1}^{r_2} \left(\frac{\omega r}{U} - \delta\right) rdr$$

$r_1 + r_2$ are the root and tip chord distances, and a rectangular fin is assumed. If $k = r_1/r_2$ and we neglect k^2 and k^3 we can integrate the preceding and obtain

$$\omega/U = \tfrac{3}{2}(\delta/r_2)$$

Substituting this into the equation for dL, we find

$$dL = C_{L_\alpha}qc\ \delta[(3r/2r_2) - 1]dr$$

The preceding equation shows that the lift distribution on a freely spinning canted fin is negative (tends to increase the spin) on inboard sections of the fin and is positive on outboard sections of the fin. Similar distributions can be obtained for other planforms once $C = f(r)$ is known. The resultant lift, which must act at the body centerline, can be computed by integrating

$$L = C_{L_\alpha}qc\ \delta(r_2/4)(4k - 1)$$

If $k = 0.1$, which is a realistic value, then the resultant lift

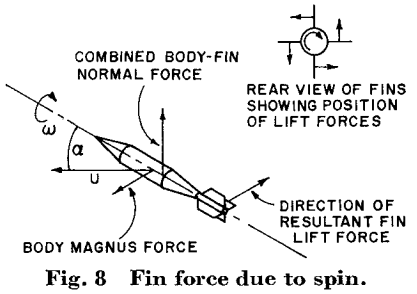

Fig. 8 Fin force due to spin.

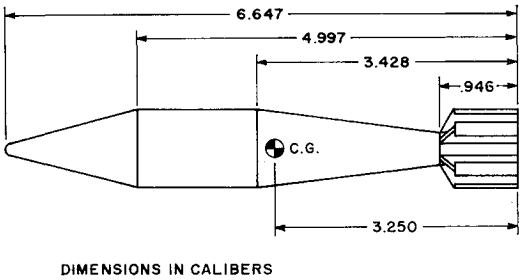

Fig. 9 Finned projectile configuration.

is approximately 15% of the lift on a nonrotating wing at angle δ. Also, the lift is in the direction of the inboard lift distribution. On a projectile having symmetrical fins the lift on opposing fins cancels so that zero lift acts on the complete configuration.

At angles of attack other than zero the rolling moment on a freely spinning finned configuration is still zero; however, the lift distribution on each fin is no longer the same. As each fin rotates through the flow on the lee side of the body, its lift distribution is altered by the body wake. At small angles of attack, only the inboard lift distribution is affected, and this, because of the symmetry about the angle-of-attack plane, will produce a force in the body Magnus force direction. At larger angles of attack, the body wake will influence the outboard lift distribution also, and the resultant force will decrease toward zero. Through this mechanism it is possible to predict a nonlinear Magnus force on a freely spinning finned projectile.

Magnus data have been obtained from experiments[13] to determine the body-fin interference on a typical fin stabilized projectile with uncanted fins (Fig. 9). Magnus data at one Mach number are shown in Fig. 10, and additional data are presented in Ref. 13. In Fig. 10 the Magnus data for both the bare body and the finned body are compared. It is seen that the bare-body Magnus force is positive, whereas the force on the finned body is negative. Therefore, the Magnus force on the fins opposes that on the body, as mentioned previously, with the fins having the larger force. The Magnus moment on the finned body is larger than that on the bare body, and is caused by the combined action of the moment couple and the resultant negative force. The effective center of pressure for this configuration is located aft of the projectile because of the couple mentioned previously.

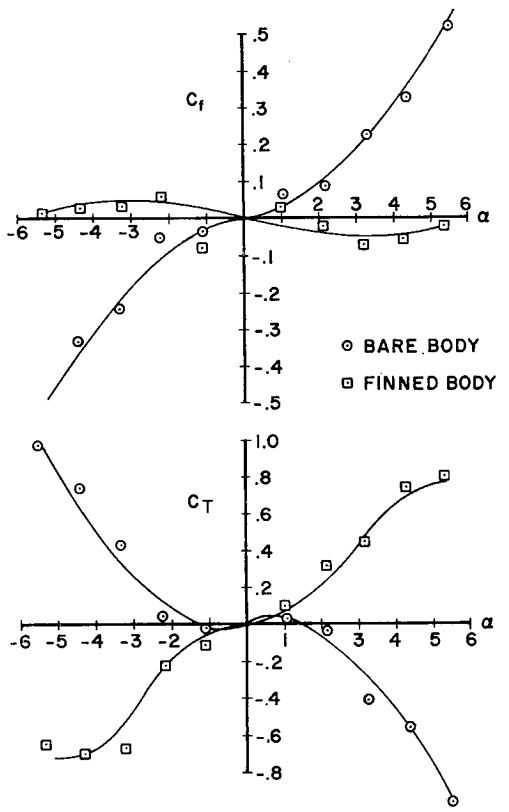

Fig. 10 Magnus characteristics of a finned projectile at $M = 2.0$, $Re = 0.65 \times 10^6$, $(\omega r/U) \leq 0.025$.

Magnus Effects Due to Canted Fins

Recently Benton[14] has shown that a Magnus moment can be created on canted fins, provided the fins are canted differentially. The moment is a couple created by a component of the fin normal force, and its origin is illustrated in Fig. 11. The moment can be determined from

$$T = -(N_1 y_1 + N_3 y_3)\delta$$

where

$$N_1 y_1 = \int_{d/2}^{3d/2} qC_{N_\alpha} \left(\alpha_B - \delta + \frac{\omega y}{U}\right) d\, y dy$$

$$N_3 y_3 = \int_{d/2}^{3d/2} qC_{N_\alpha} \left(\alpha_B + \delta - \frac{\omega y}{U}\right) d\, y dy$$

The subscripts 1 and 3 refer to the two fins. Then

$$T = -2\, qC_{N_\alpha} \alpha_B d^3 \delta$$

$$C_{T_\alpha} = -\frac{8}{\pi}\left(\frac{\omega d}{2\delta U}\right)^{-1} C_{N_\alpha}$$

It should be pointed out that the moment is a function of the fin cant angle and is independent of spin. It acts even

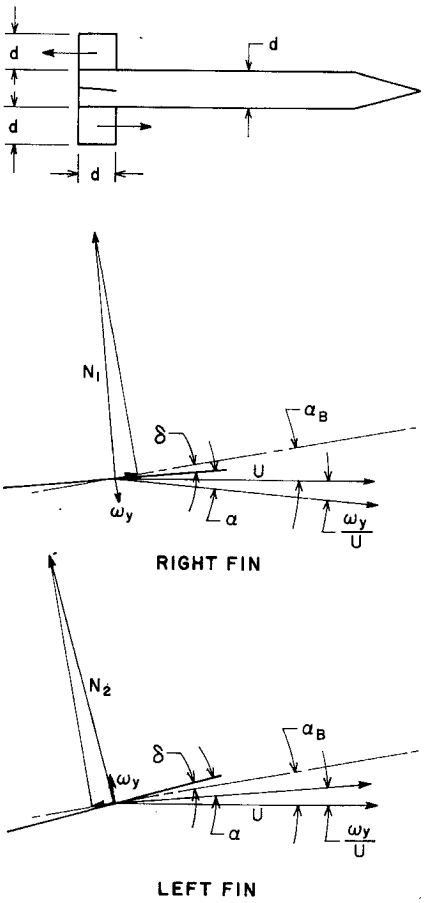

Fig. 11 Magnus moment acting on canted fins.

at zero spin, and its magnitude can be predicted once the cant angle, the fin normal force, and the fin geometry are known. Benton has computed the Magnus moment on a configuration which has been experimentally tested by MacAllister and Nicolaides.[15] The results show good agreement above $M = 2$ (Fig. 12). This moment is extremely large compared to the body fin interference moment (Fig. 10).

Magnus Effects Due to Fin Base Pressure

A Magnus moment can be established on fins, providing a laminar boundary layer exists on the fins. Chapman, Wimbrow, and Kester[16] have shown that the base pressure on a thin wing or fin ($t/c < 5\%$) can change suddenly when the following conditions are satisfied: low supersonic Mach number, low Reynolds number (laminar boundary layer), thin trailing edge, and small angles of attack (Fig. 13). The change in base pressure occurs suddenly, as the wing angle of attack reaches the critical angle. The critical angle is dependent on the Reynolds number, etc., and in the experiments conducted by Chapman et al. the critical angle varied from 1° to $3\frac{1}{2}$°. Some hysteresis was also noted in that the critical angle depended on the way in which the angle was approached. The maximum pressure change observed was from $P_b/P_\infty = 0.42$ to 0.82.

In considering the flow over a rotating finned body, the angle of attack of each two opposing fins, when the fins are perpendicular to the angle-of-attack plane, can be written as

$$\alpha_{\text{left}} = \alpha_B + \delta - (\omega y/U)$$

$$\alpha_{\text{right}} = \alpha_B - \delta + (\omega y/U)$$

From the preceding equations it is seen that the angle of attack of each fin need not be the same. Two typical examples of the fin angles of attack are shown in Fig. 14. The right and left fins are at different angles of attack and, provided the other conditions listed by Chapman et al. are met, the base pressures existing on the two opposing fin bases can be different.

The preceding equations hold only at the instant when the fins are perpendicular to the body angle-of-attack plane (fin-roll angle = 0°). At other fin-roll angles the fin angles of attack oscillate between the right- and left-hand values, thereby providing a continuously changing angle of attack on each fin. If the critical angle of attack is somewhere between the right- and left-hand values, then the fin base pressure will change as the fins rotate. With multifin configurations, at least one set of fins can be expected to have unequal base pressures as long as the Chapman conditions

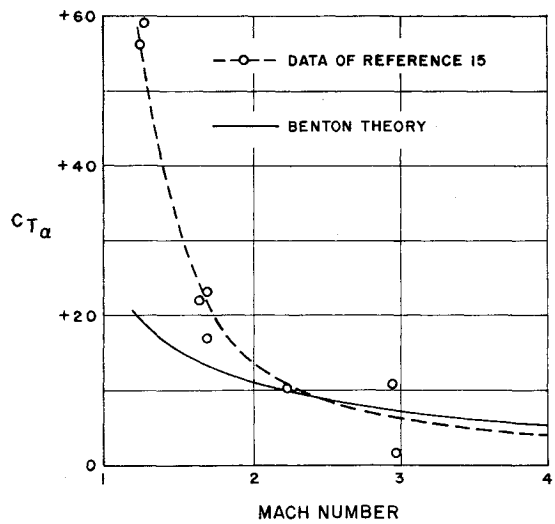

Fig. 12 Magnus moment as a function of Mach number.

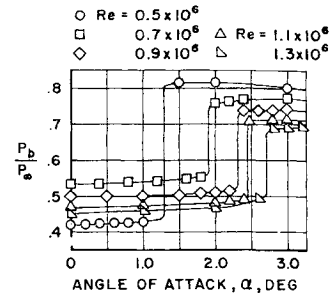

Fig. 13 Effect of angle of attack on base pressure for a thin laminar flow wing.

hold. This will create a moment that can be computed as shown below:

$$C_{T_\alpha} = \frac{[(P_b/P_\infty)_R - (P_b/P_\infty)_L]S_b b P_\infty}{q\pi(d^2/4)d(\omega d/2U)\alpha_B} = \frac{[(P_b/P_\infty)_R - (P_b/P_\infty)]S_b b}{(\gamma M^2/2)(\pi d^3/4)(\omega d/2U)\alpha_B}$$

If the two base pressures are $P_b/P_\infty = 0.82$ and 0.42, the configuration is that in Fig. 11, and the fin-thickness ratio is 5% ($S_b = 0.05\,d^2$); then

$$C_{T_\alpha} = (0.82 - 0.42)\cdot 4/\gamma M^2\,\pi(\omega d/2U)\alpha_B$$

Using the values $\gamma = 1.4$, $M = 1.5$, $\alpha_B = 2°$, and $(\omega d/2U) = 0.01$, then $C_{T_\alpha} = 0.80$. Using the values $\gamma = 1.4$, $M = 1.5$, $\alpha_B = 5°$, and $(\omega d/2U) = 0.02$, then $C_{T_\alpha} = 0.16$. The preceding values show that the base pressure moment in this case is considerably smaller than the moment due to fin cant (Fig. 12) but probably larger than the body-fin interference moments. However, the unequal base pressure moment may be an intermittent moment in that the Chapman conditions in some cases may be intermittent. In this case it would be best to eliminate this moment by tripping the boundary layer on the fin leading edges.

Also, the unequal base pressure moment cannot exist on the MacAllister-Nicolaides configuration, for the fins are 8% thick. Chapman's experiments show that fins over $7\frac{1}{2}$% thick are not subject to the sudden change in base pressure.

Conclusions

The experiments and studies during this investigation have brought to light many interesting properties of spin effects

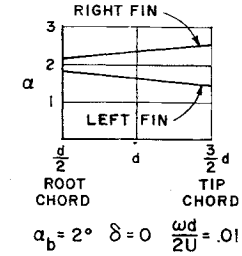

Fig. 14 Angles of attack of fins under various conditions.

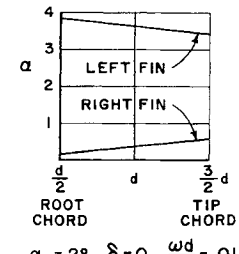

on finned and nonfinned projectiles. These properties are listed below:

1) The Magnus force and moment are the most important aerodynamic effects of spin. The normal force and pitching moment are not affected by spin.

2) For aerodynamically clean bodies of revolution, the Magnus force and moment are linear with spin and angle of attack in the low angle-of-attack range. The Magnus force center of pressure is located on the rear portion of the body.

3) The boundary-layer properties can affect the magnitude of the Magnus force at low angles of attack.

4) The Magnus force and moment on a short aerodynamically clean body having a laminar boundary layer can be predicted from Martin's theory.

5) Modifications to the surface of an aerodynamically clean body can drastically change the Magnus characteristics of the body. This may change the sign of the force, as is the case with the round base, and also make the force nonlinear with spin and angle of attack.

6) At high angles of attack, where the crossflow is transonic, the Magnus force on a body agrees quite well with the Magnus force on a cylinder flying normal to its main axis.

7) On a finned projectile, the body-fin interference produces a Magnus force and moment, which drastically change the Magnus characteristics of the configuration. This applies to both canted and uncanted fins.

8) A Magnus moment of considerable magnitude can exist on canted fins. This moment is due to components of the fin normal force acting in the drag direction.

9) A Magnus moment due to unequal fin-base pressures can exist under certain conditions. The required conditions are laminar boundary layers on the fins, low supersonic Mach number, thin fins, and low angles of attack.

References

[1] Magnus, G., "Uber die Aberwucheing der Geschosie," Abhandle. Deut. Akad. Wiss. Berlin (1852); also Poggendorff, J. C., Ann. der Physik Chem. **88**, I (1853).

[2] Thorman, H. C., "Boundary layer measurements on an axisymmetric body with spin and yaw," Guggenheim Aeronautical Laboratory, Calif. Institute of Technology Rept. on Army Contract DA-04-495-ORD-481 (November 1957).

[3] Martin, J. C., "On Magnus effects caused by the boundary layer displacement thickness on bodies of revolution at small angles of attack," Ballistic Research Laboratories Rept. 870 revised (June 1955).

[4] Kelly, H. R., "An analytical method for predicting the Magnus forces and moments on spinning projectiles," Naval Ordnance Test Station, NAVORD TM 1634 (August 1954).

[5] Kelly, H. R. and Thacker, G. R., "The effect of high spin on the Magnus force on a cylinder at small angles of attack," Naval Ordnance Test Station, NAVORD Rept. 5036 (February 1956).

[6] Platou, A. S. and Sternberg, J., "The Magnus characteristics of a 30 mm aircraft bullet," Ballistic Research Laboratories, BRL Rept. 994 (September 1956).

[7] Deitrick, R. E., "Effect of a hemispherical base on the aerodynamic characteristics of shell," Ballistic Research Laboratories, BRL Rept. 947 (November 1955).

[8] Platou, A. S., "The Magnus force on a short body at supersonic speeds," Ballistic Research Laboratories, BRL Rept. 1062 (January 1959).

[9] Allen, H. F. and Perkins, E. W., "A study of the effects of viscosity on flow over slender bodies of revolution," NACA Rept. 1048 (April 1946).

[10] Kelly, H. R., "The estimation of normal force and pitching moment coefficients for blunt-based bodies of revolution at large angles of attack," Naval Ordnance Test Station NOTS TM 998 (May 1953).

[11] Luchuk, W., "The dependence of the Magnus force and moment on the nose shape of cylindrical bodies of fineness ratio 5 at Mach No. 1.75," Naval Ordnance Test Station, NAVORD Rept. 4425 (April 1957).

[12] Platou, A. S., "The Magnus force on a rotating cylinder in transonic cross flows," Ballistic Research Laboratories, Rept. 1150 (September 1961).

[13] Platou, A. S., "The Magnus force on a finned body," Ballistic Research Laboratories, Rept. 1193 (March 1963).

[14] Benton, E. R., "Supersonic Magnus effect on a finned missile," AIAA J. **2**, 153 (1964).

[15] Nicolaides, J. D. and MacAllister, L. C., "A review of aeroballistic range research on winged and/or finned missiles," Ballistic TN 5, Bureau of Ordnance, Dept. of the Navy (1955).

[16] Chapman, D. R., Wimbrow, W. R., and Kester, R. H., "Experimental investigation of base pressure on blunt-trailing-edge wings at supersonic velocities," NACA TN 2611 (January 1952).